

Agrin Expression during Synaptogenesis Induced by Traumatic Brain Injury

M. CRISTINA FALO, THOMAS M. REEVES, and LINDA L. PHILLIPS

ABSTRACT

Interaction between extracellular matrix proteins and regulatory proteinases can mediate synaptic integrity. Previously, we documented that matrix metalloproteinase 3 (MMP-3) expression and activity increase following traumatic brain injury (TBI). We now report protein and mRNA analysis of agrin, a MMP-3 substrate, over the time course of trauma-induced synaptogenesis. Agrin expression during the successful synaptic reorganization of unilateral entorhinal cortical lesion (UEC) was compared with expression when normal synaptogenesis fails (combined fluid percussion TBI and bilateral entorhinal lesion [BEC]). We observed that agrin protein was increased in both models at 2 and 7 days postinjury, and immunohistochemical (IHC) co-localization suggested reactive astrocytes contribute to that increase. Agrin formed defined boundaries for sprouting axons along deafferented dendrites in the UEC, but failed to do so after combined insult. Similarly, Western blot analysis revealed greater increase in UEC agrin protein relative to the combined TBI+BEC model. Both models showed increased agrin transcription at 7 days postinjury and mRNA normalization by 15 days. Attenuation of synaptic pathology with the NMDA antagonist MK-801 reduced 7-day UEC agrin transcript to a level not different from unlesioned controls. By contrast, MK-801 in the combined insult failed to significantly change 7-day agrin transcript, mRNA levels remaining elevated over uninjured sham cases. Together, these results suggest that agrin plays an important role in the sprouting phase of reactive synaptogenesis, and that both its expression and distribution are correlated with extent of successful recovery after TBI. Further, when pathogenic conditions which induce synaptic plasticity are reduced, increase in agrin mRNA is attenuated.

Key words: extracellular matrix; neuroplasticity; traumatic brain injury

INTRODUCTION

A PRINCIPAL FEATURE of traumatic brain injury (TBI) is diffuse deafferentation of target neurons (Povlishock and Christman, 1995). Central nervous system (CNS) deafferentation typically induces reactive synaptogenesis (Steward, 1989); however, when deaf-

ferentation occurs in the context of TBI, the resulting interaction of excessive neuroexcitation and traumatic axonal injury significantly reduce recovery. In order to study how this interaction affects posttraumatic synaptic plasticity, we employ a rodent injury model combining neuroexcitation and hippocampal deafferentation in the same animal, reproducing components of the persistent

cognitive deficits and poor synaptic recovery of human TBI (Phillips et al., 1994). Moreover, using entorhinal cortical lesion as the deafferentation component permits direct comparison between successful, adaptive synaptogenesis, generated by unilateral entorhinal cortical lesion (UEC) alone (Steward et al., 1988), and aberrant synaptic plasticity observed when fluid-percussion TBI is combined with bilateral entorhinal cortical lesion (BEC).

While numerous molecular species interact in synaptogenesis, proteins found in the CNS extracellular matrix (ECM) and their regulatory matrix metalloproteinases (MMPs) are of interest because they influence axonal growth and long-term synaptic modification, integral to recovery (Yong et al., 2001; Dityatev and Schachner, 2003; Hsu et al., 2006). During UEC-induced synaptogenesis, ECM proteins (e.g., neurocan, brevican, phosphacan and tenascin) are distributed along deafferented dendrites and direct sprouting axons to appropriate postsynaptic sites (Brodkey et al., 1995; Deller et al., 2001). We and others have observed that MMPs targeting such ECM substrates are also up-regulated in regions undergoing synaptic plasticity (Phillips and Reeves, 2001; Szklarczyk et al., 2002; Muir et al., 2002). One of these proteinases, MMP-3 is increased within reactive neuroglia at sites of synaptogenesis (Kim et al., 2005) and is temporally correlated with shifts in expression of the ECM proteins (Falo et al., 2006). Interestingly, expression of the synaptic ECM protein agrin was reported to increase within reactive astrocytes after CNS ischemia/reperfusion injury and was cleaved in a manner consistent with MMP3 lysis (Sole et al., 2004).

Agrin was first described as a matrix protein associated with the neuromuscular junction thought to direct axon terminals to correct postsynaptic sites on the motor endplate (Smith and Hilgenberg, 2002). Subsequent studies revealed considerable detail about NH2 terminal isoforms of agrin that subservise different functions at the motor endplate depending upon distinct subcellular localization (Burgess et al., 2000). In the periphery, Schwann cells can also produce agrin and that production is increased following axotomy, both along sprouting axons and at the neuromuscular junction (Yang et al., 2001). Initial investigation of CNS agrin showed the protein localized within the basal laminae during development (Tsen et al., 1995); however, its function did not appear specifically related to cholinergic synapse formation (Kroger and Mann, 1996). A later report by Halfter et al. (1997) showed that agrin acted as a binding partner for growth factors or adhesion molecules. Such interactions may account for *in vitro* observations that agrin induces shorter, more branched axons, important for targeting local collaterals to postsynaptic spines, and generating a higher density of presynaptic proteins synap-

physin and synapsin 1 (Mantych and Ferreira, 2001). Astrocytic agrin can affect synapse number on hippocampal neurons and the microtubular structure of neurite growth cones (Tournell et al., 2006; Bergstrom et al., 2007). More recently, Hilgenberg et al. (2004, 2006) have identified membrane tyrosine kinases and the Na⁺/K⁺ ATPase complex as agrin ligands, the latter of which may be concentrated on growth cone membranes (Brines and Robbins, 1993). Studies using oligonucleotide suppression of agrin show impaired synapse development (Ferreira, 1999), and attenuated vesicle turnover, further implicating a presynaptic function (Bose et al., 2000). Transfection of agrin siRNA into rat hippocampal neurons *in vitro* resulted in reduced numbers of neurite filopodia (McCroskery et al., 2006). This functional effect of agrin is supported by the fact that it can bind FGF-2 by a heparan sulfate-dependent mechanism (Cotman et al., 1999) and regulate FGF-2-directed neurite extension within cultured neurons (Kim et al., 2003). An increase of agrin mRNA expression was also observed with excitotoxic seizure induction in the hippocampus (O'Connor et al., 1995), a paradigm which, like combined TBI+BEC, induces an aberrant form of reactive synaptogenesis.

While *in vivo* studies of trauma-induced synaptogenesis have been reported (Phillips and Reeves, 2001; Scheff et al., 2005; Thompson et al., 2006), they did not directly address agrin. The present study examined both spatial and temporal profiles of agrin expression within the deafferented hippocampus during reactive synaptogenesis induced by TBI. Using immunohistochemical (IHC), Western blot, and reverse transcription-polymerase chain reaction (RT-PCR) analysis, both protein and mRNA expression were examined, contrasting agrin response during successful adaptive synaptic plasticity (after UEC lesion) with that of aberrant maladaptive synaptic plasticity (produced by TBI+BEC insult). Here we report that agrin expression profile varies with different postinjury phases of trauma-induced synaptogenesis, and is correlated with the extent of synaptic recovery achieved.

METHODS

Experimental Animals

Male Sprague-Dawley rats (Hilltop Laboratory Animals, Inc., Scottsdale, PA) weighing 300–350 g were used in this study. Rats were randomly divided into four experimental groups: UEC ($n = 25$); TBI+BEC ($n = 29$); UEC + MK-801 treatment ($n = 4$); and MK-801-treated TBI+BEC ($n = 4$). Four paired control groups included the following: sham-injured ($n = 15$), sham-injured + MK-801 ($n = 3$); UEC + vehicle treat-

ment ($n = 4$); vehicle-treated TBI+BEC ($n = 4$); and sham-injured vehicle-treated ($n = 4$). All rats were housed in individual cages with food and water *ad libitum* in a 12-h dark-light cycle at 22°C. Animal care facilities were accredited, with full-time veterinarians and supportive staff present for supervision and consultation. All protocols for injury and use of animals were approved by the Institutional Animal Care and Use Committee.

Unilateral Entorhinal Cortical Lesion

All animals were surgically prepared under isoflurane anesthesia (2% in carrier gas of 70% N₂O and 30% O₂) delivered via a nose cone. During all surgical procedures body temperature was maintained at 37°C. Lesions were performed using a modification of the method previously described by Loesche and Steward (1977). Once under inhalation anesthesia, rats were placed in a stereotaxic frame and an area of skull was removed to expose the entorhinal cortex of the right hemisphere. A teflon-insulated wire electrode was angled at 10° from perpendicular and current passed (1.5 mA for 40 sec) at a total of nine stereotaxic sites: 1.5 mm anterior to the transverse sinus; 3, 4, and 5 mm lateral to midline; and at 2, 4, and 6 mm ventral to the brain surface. Once the procedure was completed, the electrodes were removed, the scalp was sutured closed over the surgical site, and Bacitracin applied to the wound. Animals were monitored for full recovery from anesthesia, and once able to walk and right themselves, they were returned to their home cages.

Experimental Traumatic Brain Injury

Surgical preparation. All animals were surgically prepared under isoflurane anesthesia (2% in carrier gas of 70% N₂O and 30% O₂) delivered via a nose cone. After placement in a stereotaxic frame, the scalp was sagittally incised and a 4.8-mm hole trephined into the skull over the sagittal suture, midway between bregma and lambda. Two steel screws were placed 1 mm rostral to bregma and 1 mm caudal to lambda. A modified Leur-Loc syringe hub with an inner diameter of 2.6 mm was placed over the exposed dura and bonded to the skull with cyanoacrylate adhesive. Dental acrylic was then poured around the syringe hub and skull screws, and allowed to harden. The hub was packed with Gelfoam, the scalp sutured closed and bacitracin was applied to the surgical site. Animals were monitored for full recovery from anesthesia, and once able to walk and right themselves, they were returned to their home cages.

Fluid percussion traumatic brain injury. The model used for injury was the same as that described by Dixon et al. (1987). The fluid percussion injury (FPI) device

consists of a Plexiglas cylinder 60 cm long and 4.5 cm in diameter, filled with double distilled water. The cylinder is closed at one end with a rubber-covered Plexiglas piston mounted on O rings. The opposite end of the cylinder is closed by an 8-cm metal extracranial pressure transducer (model EPN-0300-100A; Entram Devices, Inc.). Attached to the end of the metal transducer is a 5-mm tube (2.6 mm inner diameter) that terminates with a male Leur-loc fitting. This fitting is connected to the surgically implanted female Leur-Loc at the time of injury. The injury is created when a metal pendulum strikes the piston of the injury device, injecting a small volume of water into the closed cranial cavity, directly onto the exposed dura. This causes a brief (20 msec) displacement and deformation of the underlying cortex resulting in brain injury. The magnitude of the pressure pulse is recorded extracranially by an in-line transducer, expressed in atmospheres (atm) of pressure, and visualized on a storage oscilloscope (model 5111; Tektronix, Beaverton, OR). The severity of the injury is controlled by adjusting the height of the pendulum.

Twenty-four hours after the surgical preparation, rats were anesthetized with isoflurane (4% in carrier gas of 70% N₂O and 30% O₂) for 4 min in a 2-l chamber. Once anesthetized, the animals were removed from the chamber, the surgically prepared site was exposed and the animal was connected to the FPI device. Animals were injured at 2.0 ± 0.05 atm. This is equivalent to a moderate level of injury that has previously been demonstrated to produce consistent pathophysiological responses. Sham-injured controls included the same surgical preparation, anesthesia, and connection to the injury device, except that no injury was delivered. All animals were immediately ventilated until spontaneous breathing resumed, the injury site sutured closed and Bacitracin applied. Behavioral assessments were performed on the injured animal to assure a controlled level of injury, including pinna, corneal, paw, and tail reflexes, as well as righting and head support responses. Once all responses had been recorded and the animal was conscious, the injured rat was placed in a recovery chamber, monitored for any signs of bleeding, respiratory difficulty or problems with cardiovascular circulation for 2–3 h and then returned to its home cage.

Combined injury (TBI+BEC). Animals subjected to a combined injury procedure first underwent moderate (2.0 ± 0.05 atm) FPI as described above. Injured animals were returned to their home cages and 24 h later subjected to BEC lesion (Phillips et al., 1994). Lesions of the entorhinal cortex were performed on each side of the brain as indicated above for UEC cases. Once the bilateral procedure was completed, the electrodes were re-

moved, the wound site sutured closed, and Bacitracin applied. All lesioned animals were monitored for postoperative recovery of sensory and righting reflexes, after which they were returned to their home cages.

MK-801 Treatment

MK-801 was administered in a chronic treatment paradigm previously demonstrated to attenuate UEC-induced dendritic atrophy (Nitsch and Frotscher, 1992) and reduce cognitive deficits in the TBI+BEC model (Phillips et al., 1998). Fifteen minutes prior to either UEC or BEC lesion, rats were given an initial dose of 1 mg/kg MK-801 i.p. ($n = 4$ /group for UEC and TBI+BEC). This dosing was repeated twice daily for 2 days. Rats were allowed to survive for 7 days and then sacrificed as described below for RT-PCR analysis. A paired control group received drug beginning at 24 h after sham FPI ($n = 3$), matching the dosing intervals for the TBI+BEC cases. Three additional control groups ($n = 4$ each for UEC, TBI+BEC, and sham-injured) were prepared with vehicle administration. Initial statistical analysis showed that i.p. vehicle (saline) injection in injured rats had no significant effect on agrin mRNA level in either the UEC ($p = 0.313$) or TBI+BEC ($p = 0.415$) model. Accordingly, we pooled saline-treated injured rats with untreated injured rats, achieving larger (and more stable) comparison groups against which to evaluate the effect of MK-801 treatment.

Immunohistochemistry

At 2, 7, and 15 days postinjury, a subset of animals ($n = 4$ for UEC and TBI+BEC; $n = 3$ for sham-injured at each survival interval) was anesthetized with a lethal dose of sodium pentobarbital (90 mg/kg, i.p.) and transcardially perfused, first with 150 mL of isotonic saline (0.9% NaCl), followed by 500 mL of fixative (4% paraformaldehyde, in 0.1 M phosphate buffer, pH 7.2–7.4; Electron Microscopy Sciences, Fort Washington, PA). The brains were carefully removed, blocked and post-fixed in the same solution overnight at 4°C. Serial coronal vibratome sections containing bilateral mid-dorsal hippocampus were cut at 40 μ m and collected in 0.1 M phosphate buffer for free floating IHC staining using (1) an ABC method with DAB (0.05% 3,3'-diaminobenzidine dihydrochloride) visualization (Vectastain ABC Kit, Vector Laboratories) or (2) a fluorescent-labeled secondary antibody for visualization with confocal microscopy. After three 10-min washes with agitation in 0.1 M phosphate buffer (PB), pH 7.2–7.4, sections were incubated in either 10% normal serum containing 0.3% Triton X-100/0.01 M phosphate-buffered saline (PBS; pH 7.2–7.4) for 1 h at 37°C, followed by a

10-min wash in PBS for DAB processing or 0.5% H₂O₂ for 30 min, then three 10-min washes in PBS for fluorescent labeling. The tissue sections were then placed in primary antibody (agrin goat polyclonal immunoglobulin G [IgG], Santa Cruz Biotechnology; 1:500; synaptophysin mouse monoclonal, Sigma, 1:500; GFAP rabbit polyclonal IgG, Sigma, 1:2,000; CD-11 rabbit polyclonal IgG, BD Biosciences, 1:500) overnight at 4°C in either PBS for DAB or Blotto blocking buffer (0.1% Triton, PBS, fish gelatin) for fluorescence microscopy. Sections incubated without primary were processed in parallel. In each run, no DAB or fluorescent signal was observed with the minus primary controls.

After exposure to the primary antibody, DAB tissue sections were washed five times in PBS (15 min each) and subsequently incubated with a biotin-labeled secondary antibody (rabbit anti-goat) for 1 h at 37°C. After three washes in PBS (10 min each), the sections were incubated with Vectastain avidin-biotin-peroxidase reagent for 2 h at room temperature and then rinsed twice in both PBS and PB (10 min each) prior to DAB visualization of antibody binding. The DAB reaction was stopped by transferring the sections into Tris-buffered saline: two washes with agitation, 10 min each. The sections were then mounted on charged glass slides (Probe On Plus, Fischer) and allowed to dry overnight, after which they were dehydrated, cleared, and coverslipped with Permount. For fluorescent visualization, sections were washed three times in PBS (5 min each) and rinsed again in Blotto buffer prior to incubation with specific secondary antibody (rabbit anti-goat, goat anti-rabbit, or goat anti-mouse IgG) tagged by either Alexa 488 or 594 fluorescent dyes (Molecular Probes). After secondary antibody incubation, sections were rinsed in PBS for three washes each, mounted on charged glass slides in PB, and coverslipped with Vectashield. All sections were examined qualitatively for protein distribution, and images were captured using either a Nikon Optiphot light microscope or a Leica TCS-SP2 (AOBS) confocal microscope.

Western Blot

At 7 days postinjury, a subset of animals ($n = 8$ for UEC, $n = 5$ TBI+BEC, $n = 4$ for sham-injured) were anesthetized and decapitated, and hippocampi were dissected. Tissue was homogenized in cold RPER (Pierce) buffer, centrifuged at 8,000 \times g for 5 min, and supernatants collected for protein assay (Bio-Rad). Twenty micrograms of protein from each sample was mixed with reducing loading buffer (Bio-Rad), and the proteins were resolved on Bio-Rad Criterion™ 4–12% Bis-Tris gels. Protein was then transferred to PVDF membranes (Immunoblot, Bio-Rad), which were first blocked in 5%

milk + TBS-T (Tris-Buffered Saline-Tween) before being probed with antibody to agrin (goat polyclonal IgG in 5% milk + TBS-T, 1:250; Santa Cruz Biotechnology). After primary incubation, blots were washed in 5% milk + TBS-T, placed in secondary bovine anti-goat (1:20,000), and then washed in TBS-T. Signal was visualized with enhanced chemiluminescence (Super Signal®; Pierce) and imaged digitally with G: Box (Syngene) prior to densitometric analysis of band signal using Gene Tools (Syngene). Minus primary runs were performed in parallel and blots were re-probed for cyclophilin A (Upstate) to control for load variation. Injury effect was expressed as percent change relative to paired controls (contralateral side for UEC; sham-injured cases for TBI+BEC).

Semi-Quantitative RT-PCR

At 2, 7, and 15 days post-injury, a subset of animals ($n = 3-6$ for UEC, $n = 4-7$ for TBI+BEC, and $n = 6$ for sham-injured at each survival interval) was anesthetized (4% isoflurane in 70% N₂O and 30% O₂) and decapitated. Brains were rapidly removed and dissected hippocampi homogenized for RNA isolation using Trizol Reagent (Invitrogen, Carlsbad, CA). RNA was treated with DNA-free DNase Reagent (Ambion, Austin, TX), and final concentration was determined by spectrophotometry. Aliquots from each sample were then run on a 1% agarose gels containing ethidium bromide (SubCell GT System and Ready Agarose PreCast Gel System; Bio-Rad Laboratories, Hercules, CA) with 1% TBE Buffer (Invitrogen) to check for DNA contamination. Screened samples were stored at -80°C until used.

Two micrograms of the DNA-free treated rat mRNA was subjected to reverse transcription (RT) using the SuperScript First Strand Synthesis System (Invitrogen). One-tenth of the RT product was PCR amplified using a set of primers specific to rat agrin (synthesized by Bio-Synthesis, Lewisville, TX) designed according to the published rat cDNA sequence of agrin (Rupp et al., 1991). Primer pairs used for PCR amplification were as follows: 5'-CTT TGA TGG GCG GAC CTA CA-3', representing nucleotides 5490-5509; and 5'-GTC ATA GCT CAG TTG CAG GT-3' complimentary to nucleotides 5666-5685. Approximately 80 ng (1.25 μL) of template cDNA was used in each experiment. PCR samples were subjected to an initial denaturation at 94°C for 2 min, then 30 cycles of amplification (1-min denaturation at 94°C, 1-min annealing at 60°C, 1-min elongation at 72°C), followed by a final elongation at 72°C for 5 min. PCR conditions, including buffer composition and amplification cycles, were optimized in preliminary experiments. To verify amplification, 10 μL of each PCR prod-

uct was visualized with ethidium bromide on a 1% agarose gel (Ready Agarose PreCast Gel System; Bio-Rad) using a 1000-basepair (bp) DNA ladder (Invitrogen). In addition to experimental samples, negative PCR controls included samples run without cDNA template and samples not subjected to RT. Bands corresponding to the predicted cDNA bp fragments amplified by the two agrin primer pairs were excised from the agarose/ethidium bromide electrophoresed gels and sequenced (Commonwealth Biotechnologies, Richmond, VA), confirming a 99% homology to the published rat agrin cDNA profile (Rupp et al., 1991).

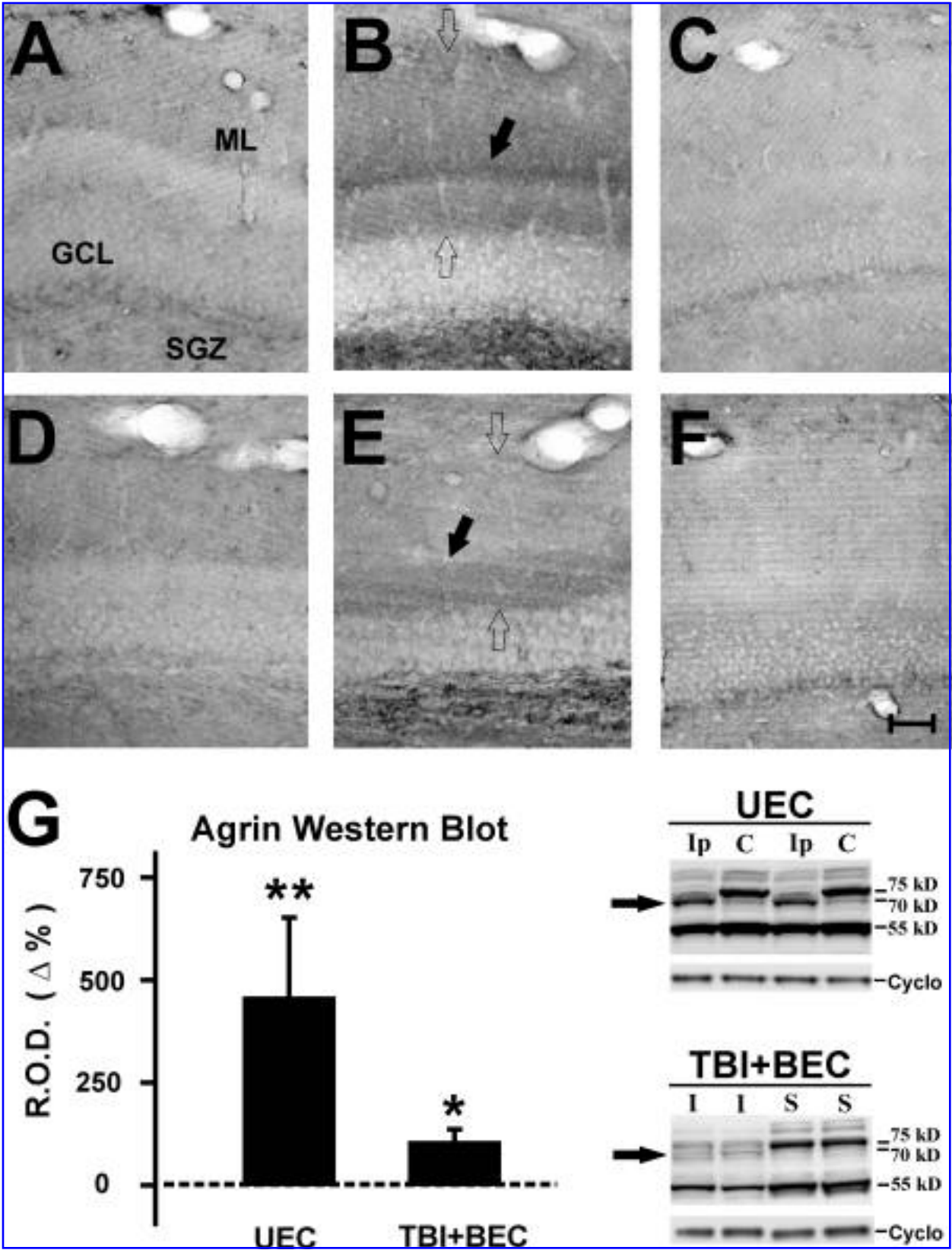
Statistical Analysis

Densitometric measures of Western blot immunobinding were analyzed for significance with the Student's *t*-test. The effects of injury and MK801 treatment on agrin mRNA levels were evaluated using analysis of variance (ANOVA), and comparisons involving specific postinjury time points were implemented using the simple main effects functions of SPSS MANOVA syntax (SPSS v11.5), which also controlled for experiment-wise error rate. The hippocampus contralateral to the entorhinal lesion served as control for the UEC model, and a separate group of sham-injured animals were used as controls for the combined injury. Data were expressed as relative change from control, and these normalized values were also used for ANOVA comparisons of mRNA changes induced by the two injury models. A probability of less than 0.05 was considered statistically significant for all experiments.

RESULTS

Agrin Immunohistochemistry

In the present study, we applied both DAB and fluorescent-labeling paradigms to track agrin expression after injury. With DAB visualization, protein distribution among deafferented dendrites could be observed in detail, particularly with respect to the laminar organization of the molecular layer (ML) during reactive synaptogenesis. By contrast, the fluorescent antibody binding technique permits co-localization of other proteins with agrin, providing more specificity as to tissue structures associated with agrin and cellular sources of agrin. In general, both DAB and immunofluorescence staining showed increased agrin protein within the dentate ML, the region specifically targeted by the deafferentation present with UEC and TBI+BEC insults, and over the subgranular zone (SGZ; Figs. 1-3). All minus primary controls failed to show immunostaining, supporting the specificity of



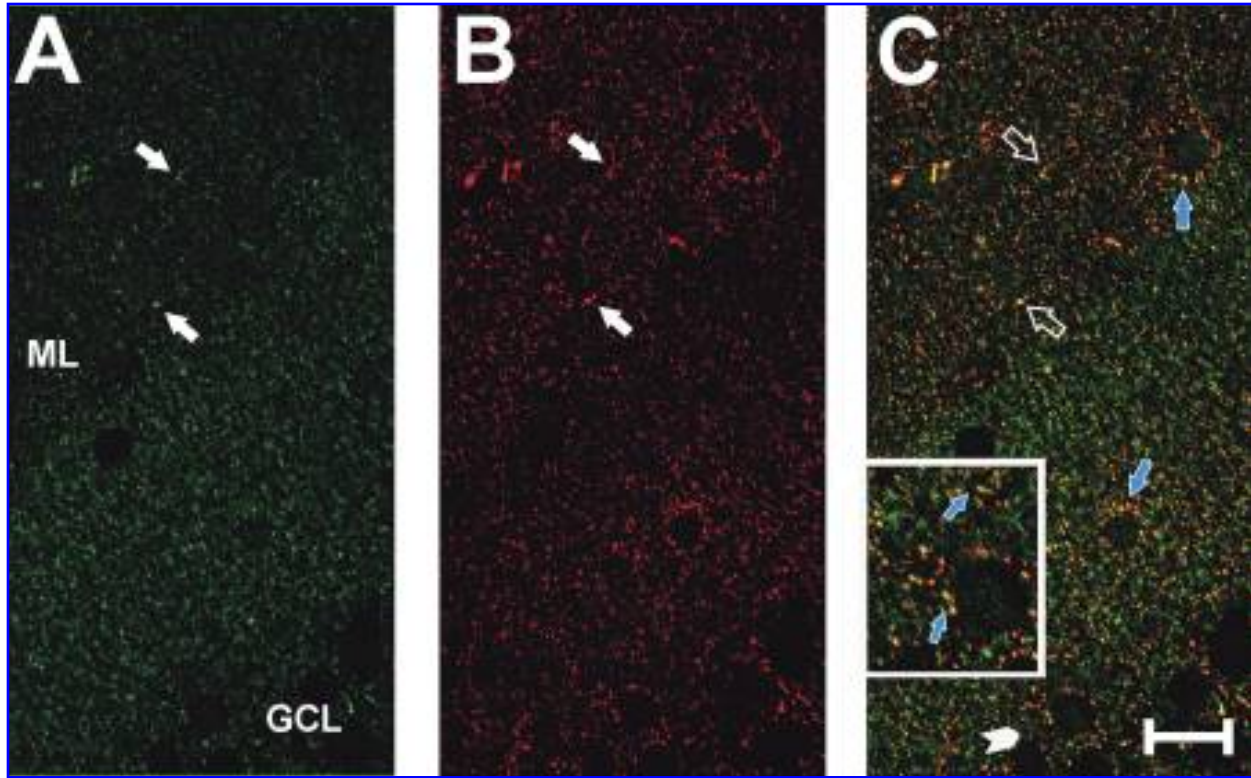


FIG. 2. Co-localization of agrin with presynaptic marker synaptophysin in deafferented dentate ML at 7 days after UEC lesion. Confocal IHC for agrin (**A**, green signal) and synaptophysin (**B**, red signal) shows punctate distribution for each protein (solid white arrows). Significant overlap of signal was observed (**C**, yellow signal; open arrows), suggesting that agrin is closely associated with sprouting presynaptic terminals. Agrin and synaptophysin co-localization was also observed at somatic synapses on ectopic granule cells (blue arrows in **C**). (**Inset in C**) Granule cell and neuropil co-localization at higher magnification (arrows; region enlarged noted by arrowhead). Scale bar = 50 μm . ML, dentate molecular layer; GCL, dentate granule cell layer.

agrin signal (data not shown). With DAB, the deafferented zone exhibited an increase in agrin at 7 days for each model (Fig. 1, open arrows in B,E). Notably, both insults produced a broad band of elevated agrin over the inner ML, however, a distinct layer of agrin deposition was observed at the interface between deafferented dendrites and the inner ML of the UEC which was not pre-

sent after combined insult (Fig. 1, black arrows in B,E). This agrin pattern emerged over time, revealing a progressive increase in the ECM protein between 2 and 7 days for each injury model. At 15 days, agrin deposition within the deafferented dentate remained elevated over that of controls, and model differences in laminar distribution persisted (data not shown). While we did not ob-

FIG. 1. Increased agrin protein in the dentate gyrus at 2 and 7 days following traumatic brain injury (TBI). (**A,B**) Increased DAB immunoreactivity for agrin within the dentate molecular layer (ML) and subgranular zone (SGZ) at 2 and 7 days, respectively, after UEC lesion. Relative to the contralateral control ML (**C**), agrin protein increases with time after injury. Agrin levels are highest in the ML at 7 days (**B**; open arrows), where a distinct band of agrin staining is observed at the interface between the inner ML and deafferented outer zone (black arrow). (**D,E**) Increased agrin labeling in the dentate ML after combined TBI+BEC insult. Compared to sham-injured control cases (**F**), agrin protein levels were also increased at 2 and 7 days (**E**; open arrows). Notably, agrin staining appears reduced overall relative to UEC, and in the region between inner and outer ML (black arrow), no distinct band of agrin was observed. Western blots at 7 days after UEC and TBI+BEC (**G**) identified three major agrin bands (75, 70, and 55 kD). The UEC hippocampus showed a fourfold increase of the 70-kD species (arrow) when compared with the contralateral side, while the same band was increased less than twofold over sham after combined insult (arrow). Scale bar = 100 μm . * $p < 0.01$; ** $p < 0.001$. ML, dentate molecular layer; GCL, dentate granule cell layer; SGZ, subgranular zone; Ip, ipsilateral to lesion; C, contralateral to lesion; I, combined insult injury; S, sham-injured.

serve any significant elevation around the vasculature within the injured neuropil, immunopositive regions were visible adjacent to the larger vessels within the ML and along the hippocampal fissure.

Western blot analysis of whole hippocampal extracts also revealed that agrin expression was altered after TBI. Three major immunopositive bands were observed, at 75, 70, and 55 kD (Fig. 1G), with only minor signal at the predicted full length 200-kD form of agrin (data not shown). Of the three major agrin species, the 70 kD showed significant change over control after injury, increasing four fold ($p < 0.001$) ipsilateral to UEC lesion and less than twofold ($p < 0.01$) in the TBI+BEC samples (Fig. 1G). While our samples were not enriched for dentate ML, changes in the 70-kD form of agrin parallel the relative differences in agrin IHC signal when the two injury models are compared. Specifically, the increase in ML tissue staining was more robust in the UEC cases. The increase in a slightly shifted agrin kD may reflect some form of lysis, however, our results failed to show significant signal in gel bands at either the 135-kD zone, or the 90- and 22-kD gel regions, sites predicted for MMP-3 and neurotrypsin proteolytic fragments, respectively (data not shown). These results suggest that agrin protein increases within regions where axonal sprouting supports reactive synaptogenesis, and the form of agrin which influences this process may be different from the full-length protein.

In the immunofluorescent labeling experiments, confocal images from the UEC confirmed the DAB increase in agrin deposition within the ML at 7 days after injury and further revealed the punctate nature of that distribution (Fig. 2A). When tissue was double labeled with antibodies against both agrin and the presynaptic protein synaptophysin, many of the punctate agrin-positive sites showed co-localization with synaptophysin (Fig. 2B,C, inset). These results suggest that a portion of neuropil agrin can be differentially distributed at or near synaptic junctions. Subsequent confocal experiments paired agrin with markers for astrocyte (GFAP antibody) and microglial (CD-11 antibody) cells in the deafferented ML at 7 days post-UEC (Fig. 3). In this case, we observed similar patterns of punctate agrin labeling (Fig. 3A), but found that areas of more concentrated agrin deposition were localized within GFAP-positive astrocytes (Fig. 3B,C). By contrast, tissues exposed to agrin and microglial antibody failed to show cell body co-localization of the two markers (Fig. 3D, open arrows, inset), and suggested that microglial movement within the deafferented zone may be restricted at the high agrin boundary of the inner ML (Fig. 3D, solid bar). Together these observations support local production of agrin by reactive astrocytes during synaptogenesis and its direct association

with presynaptic terminals in the region of axonal sprouting and synaptogenesis.

Agrin mRNA Expression

As an initial approach, we compared the time course of hippocampal agrin transcription during UEC adaptive synaptic recovery with the maladaptive TBI+BEC insult using semi-quantitative RT-PCR methods. For both UEC and the combined insult, injury induced a similar temporal shift in agrin mRNA relative to paired controls and comparison of transcript levels between models showed no significant difference for any time period (Fig. 4). At 7-day survival, during the period of collateral sprouting and rapid synaptogenesis, agrin mRNA expression was significantly elevated in both the UEC (39.2% over contralateral, $p < 0.01$) and TBI+BEC (45.4% over sham-injured, $p < 0.01$) groups (Fig. 4A,B). By contrast, the earlier 2-day interval showed no significant change in agrin mRNA for either injury; however, agrin mRNA was 4.6% higher than sham-injured cases in the maladaptive TBI+BEC model suggesting a trend toward difference from UEC. Given that primary axonal degeneration and debris removal occurs during the 2-day survival interval (Phillips and Reeves, 2001; Eyupoglu et al., 2003), increased transcription of extracellular proteins like agrin, which may be reorganized to facilitate axonal outgrowth, would not be predicted. Similarly, the two models showed no significant difference in agrin transcription at 15 days postinjury, the period of recovery when the rate of synapse formation tends to plateau and pruning of synapses occurs. Notably, 15-day agrin mRNA remained 8% higher than sham-injured controls after TBI+BEC. Thus, overall agrin gene expression in the combined insult suggests a trend toward persistent elevation of the matrix protein, consistent with its role in synapse formation (Nitkin et al., 1987; Koulen et al., 2002; Cohen-Cory, 2002).

MK-801 Treatment and Agrin mRNA Expression

Our present immunohistochemical and RT-PCR analyses showed that agrin expression can vary as a function of time during synaptic recovery. To test the importance of agrin during synaptic recovery, we assessed its transcription in animals subjected to treatment with the NMDA antagonist MK-801, which has been shown to reduce damage and enhance recovery in these models. MK-801 treatment reduces dendritic pathology after UEC deafferentation (Nitsch and Frotscher, 1992) and improves functional recovery in the combined injury model (Phillips et al., 1998). The effect of MK-801 treatment on agrin mRNA expression was assessed at 7 days post-injury because that time point marks the onset of synap-

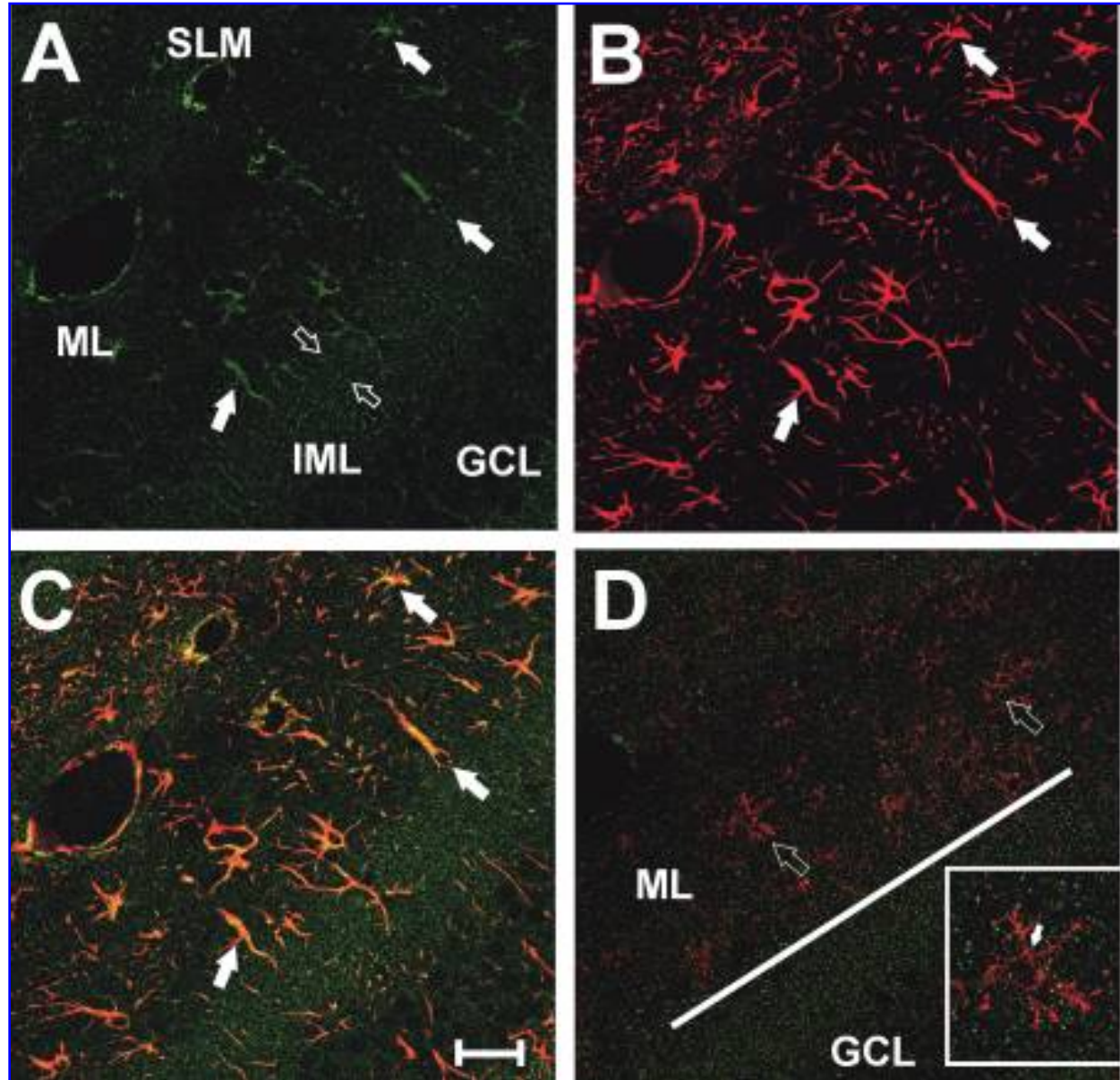


FIG. 3. Distribution of agrin with respect to reactive astrocytes and microglia in the dentate ML at 7 days after UEC lesion. (A) Confocal IHC shows agrin (green signal) as punctate profiles throughout the dendritic zone, with a higher density in the inner ML marking the interface between that layer and the outer, deafferented zone (open arrows). Within the outer ML, high agrin labeling occurs in regions suggestive of cell body and process profiles (solid arrows). (B) Multiple reactive astrocytes (arrows) within in the deafferented outer ML, their processes filled with GFAP (red signal). (C) Overlay image shows that agrin is present within these reactive astrocytes (yellow signal). (D) CD-11 positive microglia (red signal) in the same zone (open arrows), notably failing to extend their processes beyond the inner ML interface where agrin (green signal) density is high (solid line). (Inset in D) Enlarged view of microglial cell at open arrow. In contrast to the astrocytic co-localization of agrin and GFAP, agrin was not found within the CD-11 positive cell bodies of microglia (arrow). The majority of agrin positive puncta failed to overlap with CD-11 signal, however, isolated co-localization was sometimes observed along glial processes, likely sites of phagocytosed synapses. Scale bar = 100 μ m. ML, dentate molecular layer; IML, inner molecular layer; GCL, dentate granule cell layer; SLM, stratum lacunosum moleculare.

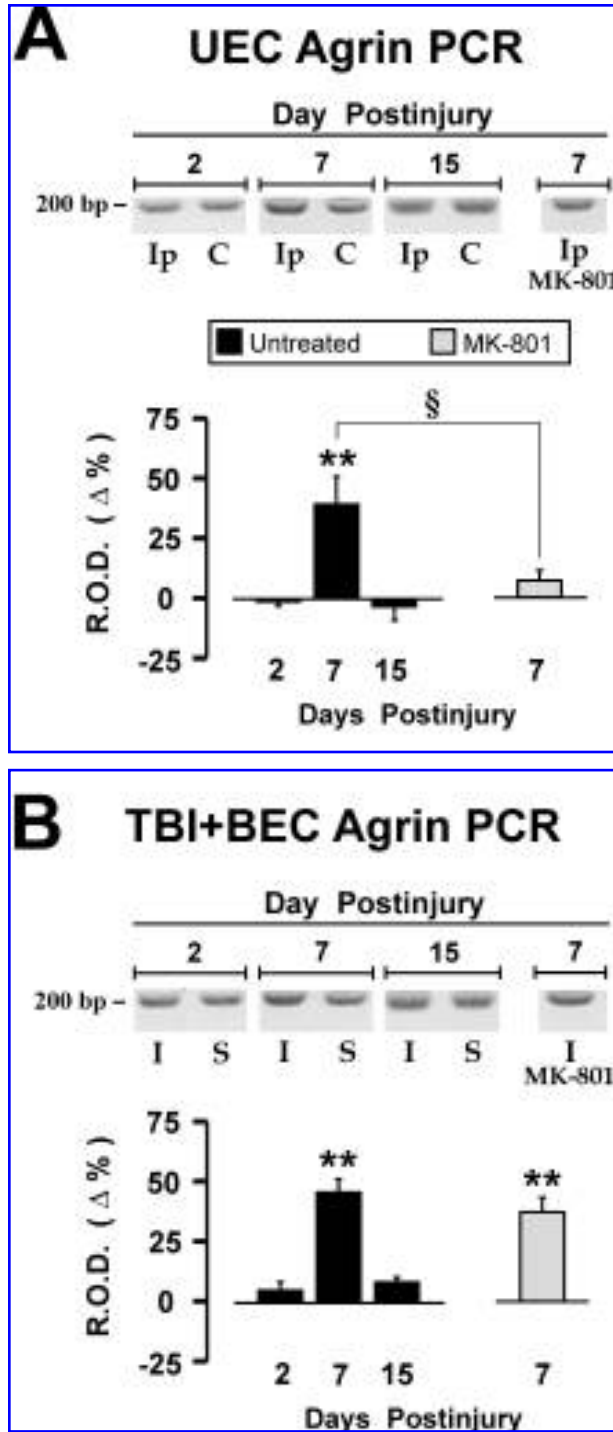


FIG. 4. Hippocampal agrin mRNA expression following traumatic brain injury (TBI) and the effect of NMDA antagonism on agrin transcript. Relative amount of mRNA is expressed as percent of contralateral side for UEC and percent of sham-injury for TBI+BEC, with control level denoted as 0% line. Both UEC (A) and TBI+BEC (B) show an elevation of agrin message at 7 days postinjury (39.2% after UEC and 45.4% after TBI+BEC), which returned to control levels by 15 days. Comparison of agrin transcript between injury models showed no significant difference for any time period. With MK-801 treatment, the UEC showed significant reduction in agrin mRNA relative to untreated lesioned, reaching a level not different from unlesioned controls. In contrast, MK-801 treatment did not significantly reduce PCR product relative to untreated injured cases and transcript level in treated animals remained elevated relative to sham controls. (Insets in A,B) Representative agarose gel profiles of agrin PCR products. Ip, ipsilateral to lesion; C, contralateral to lesion; I, combined insult injury; S, sham injured. ** $p < 0.01$ (injured vs. paired control); § $p < 0.05$ (untreated 7-day vs. MK-801 treated).

nificantly attenuated ipsilateral agrin mRNA expression by 32% ($p < 0.05$; Fig. 4A), reducing agrin transcription to a level which was not significantly different from contralateral control. By contrast, TBI+BEC cases treated with MK-801 had agrin mRNA levels only 8% lower than untreated injured cases, a difference which was not significant ($p = 0.208$; Fig. 4B). Agrin transcript in the combined treated cases remained significantly elevated over sham controls ($p < 0.01$). No statistical difference in agrin mRNA was detected between sham-saline and sham-MK-801 treated groups (data not shown). These results indicate that when deafferentation-induced pathology is reduced, agrin gene expression during periods of axonal sprouting is also reduced. Further, if deafferentation is combined with neuroexcitatory insult, the effect of NMDA antagonism on agrin transcription is blunted, suggesting that the role of NMDA linked pathways in reactive synaptogenesis varies as a function of the pathology present.

DISCUSSION

Here we describe the spatio-temporal profile of agrin protein and mRNA expression in adult rat hippocampus following TBI. Two different injury models were compared: one exhibiting successful synaptic reorganization (UEC lesion) and the other poor synaptic recovery (TBI+BEC insult). Each model was probed for agrin expression over the first 15 d after injury, focusing on the deafferented hippocampal formation. We report that (1) agrin protein increased in sub-regions targeted by injury,

togenesis, and is the survival interval where we observed elevated agrin transcript and increased agrin protein over the deafferented dentate ML.

RT-PCR analysis of 7-day hippocampal agrin mRNA expression after MK-801 treatment is shown in Figure 4. Relative to untreated UEC cases, NMDA antagonism sig-

a response associated with synaptic terminals and local reactive astrocytes, (2) postinjury agrin protein was reduced and diffusely distributed in the poorly recovering model, (3) agrin mRNA expression was increased within both models during the period of rapid synapse formation, and (4) NMDA antagonism significantly attenuated agrin mRNA following adaptive synaptogenesis, but did not alter agrin transcript during maladaptive plasticity. Overall, these observations identify distinct spatial and temporal differences in agrin expression which are associated with the efficacy of synaptic plasticity.

While the finding of injury-induced change in agrin is not surprising, the present study is the first to identify the specific phase of reactive synaptogenesis most influenced by agrin and suggests that distribution of agrin affects the extent of synaptic reorganization. Both the adaptive and maladaptive models of hippocampal plasticity showed time-dependent alterations in agrin protein and mRNA. At 2 days postinjury, IHC revealed an increase in hippocampal agrin protein diffusely distributed over the deafferented dentate ML. Confocal microscopy associated agrin with synaptophysin-positive presynaptic terminals, which is consistent with agrin enrichment in hippocampal synaptosomal fractions (Bose et al., 2000). At 7 days postinjury, model-related agrin differences became pronounced. Although both models exhibited further increases within the inner ML and hilar SGZ, only the adaptive UEC model had a distinct agrin band at the middle/inner ML interface, the border between deafferented and intact dendritic laminae. Agrin was co-localized with GFAP marking reactive astrocytes along the middle/inner ML boundary, suggesting that astrocytic agrin contributes to the concentrated band seen with IHC. We also found that activated microglia did not cross this agrin boundary, remaining within the zone of terminal degeneration, suggesting that agrin may orient activated microglia for debris removal and delineate dendritic layers targeted to receive collateral sprouts. Agrin may function like the proteoglycans neurocan and brevican, which have been posited to direct presynaptic terminals toward appropriate targets as synapses regenerate (Deller et al., 2001). Such regulation could occur through reactive astrocytes in a synaptic field where neuronal forms of agrin are in transition, as was suggested from studies of agrin mutant mice (Serpinskaya et al., 1999).

Western blot analysis of 7-day postinjury hippocampus did not show agrin proteolysis during reactive synaptogenesis. Our prior studies with TBI+BEC documented persistent MMP3 elevation in the maladaptive combined insult at 7-day postinjury (Kim et al., 2005; Falo et al., 2006), an effect which we posited may underlie abnormal lysis of matrix substrates such as agrin. In the present study, only minor expression of the full-length 200-

kD form of agrin was observed, and the 135-kD proteolytic fragment produced by MMP3 (Sole et al., 2004) was not detected. A report by Reif et al. (2007) shows that agrin is also lysed by neurotrypsin, generating a major 22-kD fragment. Similarly, that fragment was not observed in our samples, suggesting that proteolysis may not be a primary regulator of agrin expression during trauma-induced synapse reorganization. By contrast, we found that agrin was expressed as three low-molecular-weight species of 55–75 kD. UEC lesion induced a four fold increase in one of these forms, which could underlie the strong band of agrin at the inner/middle ML observed at 7 days with IHC. After combined insult, the same agrin form was increased only twofold and the inner/middle ML band of agrin no longer visible, results consistent with persistent MMP3 elevation reported at 7 days after TBI+BEC (Falo et al., 2006). Similar 55–75-kD species were observed in the characterization of brain agrin (Godfrey, 1991). More recent studies suggest multiple CNS agrin isoforms, some of which are glial specific (Kroger and Schroder, 2002), and may mediate establishment of hippocampal synapses (Tournell et al., 2006). Given these observations, it is possible that reactive astrocytes secrete agrin within the ML to facilitate synapse repair following TBI. In fact, 55–75-kD agrin species are secreted extracellularly within the developing visual system (Denzer, et al., 1995; Tsen et al., 1995). While we cannot rule out the possibility that the altered 55–75-kD forms are intermediate proteolytic products, this seems unlikely since we failed to observe the major MMP3- or neurotrypsin-generated peptide fragments.

In parallel RT-PCR analysis, we found that injury increased agrin mRNA during both adaptive and maladaptive plasticity. Consistent with our protein data, we observed a significant increase in agrin transcript at the 7-day period of active sprouting and synaptogenesis. No changes in mRNA were detected at either 2 or 15 days post-injury. This pattern suggests that agrin transcription and translation are linked temporally, responding maximally during periods of presynaptic terminal growth. In fact, when agrin expression is blocked *in vitro*, synaptogenesis on hippocampal neurons is severely attenuated (Bose et al., 2000). Such a response parallels ciliary ganglion innervation, where agrin mRNA is increased within supportive neuroglia during neurite extension and synaptogenesis (Thomas et al., 1993). In the present models, terminal degeneration is extensive at 2 days, but not at 7 days. During this early degenerative phase matrix protein scaffolds are likely altered to permit a more malleable extracellular space. While IHC did show a modest agrin increase at 2 days, RT-PCR results suggest that early shifts are more likely related to change in mRNA translation rather than significant transcriptional effects. At 15

days after injury, regenerated synapses undergo selective pruning and stabilization, a process also requiring structural flexibility around synapses. While modest changes in agrin would also be predicted for this phase of recovery, it should be noted that shifts in agrin mRNA during synapse formation may be a complex response. For example, Lesuisse et al. (2000) suggest that agrin isoforms either increase or decrease depending upon synapse maturity or activity, and Li et al. (1999) reported that non-neuronal agrin mRNA was sufficient for synapse maturation. In this context, the present study shows prominent increase of agrin protein within reactive glia during synapse reconstruction. Alternatively, it may be that changes in 7-day agrin mRNA level are indirectly affected by increases in MMP expression and enzyme activity occurring as early as 2 days postinjury (Phillips and Reeves, 2001). If these enzymes target agrin immediately after injury, agrin levels would be dampened acutely, possibly driving increased agrin transcription at 7-day survival.

In the present study, NMDA receptor antagonism with MK-801 did reduce agrin mRNA expression; however, the extent of this reduction was different between the two injuries. For these experiments, we implemented a MK-801 dosing paradigm shown to affect recovery in both models. Nitsch and Frotscher (1992) showed that MK-801 treatment of UEC attenuated dendritic atrophy, an effect linked to the reduced expression of c-fos, which moderated activation of downstream cytoskeletal genes. Together, these UEC changes led to reduced cellular damage from deafferentation which would enhance recovery. Using a similar MK-801 paradigm, we reported that NMDA antagonism could stabilize synaptic cytoarchitecture and partially restore cognitive function in the combined insult model (Phillips et al., 1998). Overall, the current study shows a strong effect of NMDA antagonism on agrin gene expression in the UEC model, but only a slight shift toward lower expression after TBI+BEC insult. These results indicate that agrin response during synaptic reorganization is associated with NMDA signaling pathways, and that agrin is a mediator of the beneficial effects of NMDA antagonism during UEC synaptogenesis. However, from the observed model differences, we conclude that the effect of NMDA antagonism on agrin expression depends, in part, upon the type of deafferentation pathology which induces synaptic plasticity. For example, the primary UEC pathology is loss of excitatory perforant path input to granule cell dendrites, while the excessive neuroexcitation of combined insult also produces hilar cell death, generating a second deafferentation and further alteration of NMDA activation. One direct interpretation would be that differences in the level of NMDA-driven Ca^{2+} signaling un-

derlie the agrin response, the combined insult producing much greater Ca^{2+} -mediated gene expression. This view is supported by studies of excitatory insult associated with CNS trauma (Yoshimura et al. 2003), kainic acid seizures (Hilgenberg et al., 2002), and hilar-lesion epilepsy (O'Connnor et al., 1995), all of which document shifts in agrin expression. Such excitatory depolarization elevates intracellular Ca^{2+} , increasing the level of transcription factors like c-fos, which can activate agrin mRNA production. With strong transcription signals in play after TBI+BEC, the positive effects of NMDA antagonism may be outweighed and MK-801 treatment only partially effective. It would be interesting to establish if a more protracted treatment with MK-801 in the combined insult increases the extent of synaptic recovery and normalizes the expression of agrin mRNA in manner similar to that observed in the UEC model.

Another possible explanation for why MK-801 generated a different effect on agrin transcription in the TBI+BEC model is linked to the hilar cell death produced by TBI neuroexcitation. Loss of hilar mossy cells would result in a second ML deafferentation, removing excitatory input to the proximal dendrites of dentate granule cells. In response, granule cell axons send robust collateral innervation back to local inner ML inhibitory neurons, a recurrent circuitry which is not present in the UEC. As with hilar-lesion epilepsy, this aberrant circuitry produces a delayed hyper-inhibition (Frotscher et al., 2006). Such elevation of inhibitory drive can increase agrin transcription (Lesuisse et al., 2000), and thereby increase agrin at sites of aberrant granule cell sprouting. Indeed, we found the increase in agrin protein to be predominant over the inner ML of the combined insult, an effect which persisted up to 15 days after injury. Thus, additional inhibition within granule cell circuitry may underlie the model differences in response to MK-801. In the present study, drug administration was begun just prior to entorhinal lesion. For the UEC, MK-801 would be present to affect any lesion-induced afferent drive throughout the entire dentate circuitry, including the normally innervated inhibitory neurons. The result would be a significant attenuation of agrin gene expression. With the combined insult, neuroexcitatory injury occurs first, 24 h before exposure to drug. In this case, processes leading to aberrant inhibitory drive would be underway before NMDA antagonism, potentially shifting agrin transcription to a level not significantly altered by our MK-801 dosing paradigm. A simple way to test whether such inhibitory control of agrin expression is relevant to successful synaptic recovery would be to selectively apply MK-801 during the period of neuroexcitatory insult in the combined model. If the inhibitory thesis is correct, agrin mRNA should be reduced significantly.

Collectively, the present findings suggest that agrin plays an important role in successful synaptic reorganization after TBI. Two trauma models with marked differences in synaptic recovery showed distinct spatial and temporal changes in agrin expression after injury. The most pronounced differences were observed in agrin protein, where its tissue localization appeared to define ML boundaries as guidance for regenerating presynaptic terminals after UEC. Our results also suggest that reactive astrocytes may contribute to such agrin boundaries in the denervated neuropil. By contrast, the severely attenuated synaptic recovery of TBI+BEC produced only a modest change in the same agrin species and showed no evidence of agrin boundary formation in the ML. Another difference between the models was the persistent elevation of inner ML agrin protein with the combined insult, possibly a consequence of hilar cell death and inner ML deafferentation. The mechanism underlying recovery dependent differences in agrin mRNA was not as clear. While the time course and level of agrin transcript was similar for both good and poor synaptic recovery, our experiments showed that NMDA-mediated regulation of agrin transcription is different, and perhaps less efficient, in the model of maladaptive plasticity. Together, these model differences further support the thesis that the more complex, interactive pathologies of TBI can induce an abnormal profile of matrix proteins, resulting in aberrant synaptic reorganization and poor recovery. Future research will no doubt focus on agrin and the details of these cellular mechanisms in order to facilitate synaptogenesis after TBI.

ACKNOWLEDGMENTS

We gratefully acknowledge the expert technical assistance of Nancy Lee, Raiford Black and Lesley Harris. This study was supported by the NIH (research grant NS-44372 to L.L.P.) and Virginia Commonwealth Neurotrauma Initiative Award (grant 07-302F to T.M.R.). Microscopy was performed at the VCU Department of Anatomy and Neurobiology Microscopy Facility (supported, in part, with funding from NIH-NINDS Center P30 core grant NS-047463).

AUTHOR DISCLOSURE STATEMENT

No conflicting financial interests exist.

REFERENCES

Bergstrom, R.A., Sinjoanu, R.C., and Ferreira, A. (2007). Agrin induced morphological and structural changes in growth

cones of cultured hippocampal neurons. *Neuroscience* **149**, 527–536.

Bose, D.M., Dike, Q., Bergamaschi, A., Gravante, B., Bossi, M., Villa, A., Rupp, F., and Malgaroli, A. (2000). Agrin controls synaptic differentiation in hippocampal neurons. *J. Neurosci.* **20**, 9086–9095.

Brines, M.L., and Robbins, R.J. (1993). Cell-type specific expression of Na⁺/K⁺-ATPase catalytic subunits in cultured neurons and glia: evidence for polarized distribution in neurons. *Brain Res.* **631**, 1–11.

Brodkey, J.A., Laywell, E.D., O'Brien, T.F., Faissner, A., Stefansson, K., Dorries, H.U., Schachner, M., and Steindler, D.A. (1995). Focal brain injury and up-regulation of a developmentally regulated extracellular matrix protein. *J. Neurosurg.* **82**, 106–112.

Burgess, R.W., Skarnes, W.C., and Sanes, J.R. (2000). Agrin isoforms with distinct amino termini: differential expression, localization, and function. *J. Cell Biol.* **151**, 41–52.

Cohen-Cory, S. (2002). The developing synapse: construction and modulation of synaptic structures and circuits. *Science* **298**, 770–776.

Cotman, S.L., Halfter, W., and Cole, G.J. (1999). Identification of extracellular matrix ligands for the heparan sulfate proteoglycan agrin. *Exp. Cell Res.* **249**, 54–64.

Deller, T., Haas, C.A., and Frotscher, M. (2001). Sprouting in the hippocampus after entorhinal lesion is layer-specific but not translaminal: which molecules may be involved? *Restor. Neurol. Neurosci.* **19**, 159–167.

Denzer, A.J., Gesemann, M., Schumacher, B., and Ruegg, M.A. (1995). An amino-terminal extension is required for the secretion of chick agrin and its binding to extracellular matrix. *J. Cell Biol.* **131**, 1547–1560.

Dityatev, A., and Schachner, M. (2003). Extracellular matrix molecules and synaptic plasticity. *Nat. Rev. Neurosci.* **4**, 456–468.

Dixon, C.E., Lyeth, B.G., Povlishock, J.T., Findling, R.L., Hamm, R.J., Marmarou, A., Young, H.F., and Hayes, R.L. (1987). A fluid percussion model of experimental brain injury in the rat. *J. Neurosurg.* **67**, 110–119.

Eyupoguli, I.Y., Bechmann, I., and Nitsch, R. (2003). Modification of microglia function protects from lesion-induced neuronal alterations and promotes sprouting in the hippocampus. *FASEB J.* **17**, 1110–1111.

Falo, M.C., Fillmore, H.L., Reeves, T.M., and Phillips, L.L. (2006). MMP-3 expression profile differentiates adaptive and maladaptive synaptic plasticity induced by traumatic brain injury. *J. Neurosci. Res.* **84**, 768–781.

Ferreira, A. (1999). Abnormal synapse formation in agrin-depleted hippocampal neurons. *J. Cell Sci.* **112**, 4729–4738.

Frotscher, M., Jonas, P., and Sloviter, R.S. (2006). Synapses formed by normal and abnormal hippocampal mossy fibers. *Cell Tissue Res.* **326**, 361–367.

- Godfrey, E.W. (1991). Comparison of agrin-like proteins from the extracellular matrix of chicken kidney and muscle with neural agrin, a synapse organizing protein. *Exp. Cell Res.* **195**, 99–109.
- Halfter, W., Schurer, B., Yip, J., Yip, L., Tsen, G., Lee, J.A., and Cole, G.J. (1997). Distribution and substrate properties of agrin, a heparan sulfate proteoglycan of developing axonal pathways. *J. Comp. Neurol.* **383**, 1–17.
- Hilgenberg, L.G.W., Ho, K.D., Lee, D., O'Dowd, D.K., and Smith, M.A. (2002). Agrin regulates neuronal responses to excitatory neurotransmitters in vitro and in vivo. *Mol. Cell. Neurosci.* **19**, 97–110.
- Hilgenberg, L.G.W., Su, H., Gu, H., O'Dowd, D.K., and Smith, M.A. (2006). A $3\text{Na}^+/\text{K}^+$ -ATPase is a neuronal receptor for agrin. *Cell* **125**, 359–369.
- Hsu, J.Y., Mckeon, R., Goussev, S., Werb, Z., Lee, J.U., Trivedi, A., and Noble-Haeusslein, L.J. (2006). Matrix metalloproteinase-2 facilitates wound healing events that promote functional recovery after spinal cord injury. *J. Neurosci.* **26**, 9841–9850.
- Kim, H.J., Fillmore, H., Reeves, T.M., and Phillips, L.L. (2005). Elevation of hippocampal MMP-3 expression and activity during trauma-induced synaptogenesis. *Exp. Neurol.* **192**, 60–72.
- Kim, M.J., Cotman, S.L., Halfter, W., and Cole, G.J. (2003). The heparan sulfate proteoglycan agrin modulates neurite outgrowth mediated by FGF-2. *J. Neurobiol.* **55**, 261–277.
- Koulen, P., Honig, L.S., Fletcher, E.L., and Kroger, S. (1999). Expression, distribution and ultrastructural localization of the synapse-organizing molecule agrin in the mature avian retina. *Eur. J. Neurosci.* **11**, 4188–4196.
- Kroger, S., and Schroder, J.E. (2002). Agrin in the developing CNS: new roles for a synapse organizer. *News Physiol. Sci.* **17**, 207–212.
- Kroger, S., and Mann, S. (1996). Biochemical and functional characterization of basal lamina-bound agrin in the chick central nervous system. *Eur. J. Neurosci.* **8**, 500–509.
- Lesuisse, C., Qui, D., Bose, C.M., Nakaso, K., and Rupp, F. (2000). Regulation of agrin expression in hippocampal neurons by cell contact and electrical activity. *Mol. Brain Res.* **81**, 92–100.
- Li, Z., Hilgenberg, L.D.K., O'Dowd, D.K., and Smith, M.A. (1999). Formation of functional synaptic connections between cultured cortical neurons from agrin-deficient mice. *J. Neurobiol.* **39**, 547–557.
- Loesche, J., and Steward, O. (1977). Behavioral correlates of denervation and reinnervation of the hippocampal formation of the rat: recovery of alternation performance following unilateral entorhinal cortical lesions. *Brain Res. Bull.* **2**, 31–39.
- Mantych, K.B., and Ferreira, A. (2001). Agrin differentially regulates the rates of axonal and dendritic elongation in cultured hippocampal neurons. *J. Neurosci.* **21**, 6802–6809.
- McCroskery, S., Chaudhry, A., Lin, L., and Daniels, M.P. (2006). Transmembrane agrin regulates filopodia in rat hippocampal neurons in culture. *Mol. Cell. Neurosci.* **33**, 15–28.
- Muir, E.M., Adcock, K.H., Morgenstern, D.A., Clayton, R., Von Stillfried, N., Rhodes, K., Ellis, C., Fawcett, J.W., and Rogers, J.H. (2002). Matrix metalloproteinases and their inhibitors are produced by overlapping populations of activated astrocytes. *Brain Res. Mol. Brain Res.* **100**, 103–107.
- Nitkin, R.M., Smith, M.A., Magill, C., Fallon, J.R., Yao, Y.M., Wallace, B.G., and McMahan, U.J. (1987). Identification of agrin, a synaptic organizing protein from *Torpedo electric organ*. *J. Cell Biol.* **105**, 2471–2478.
- Nitsch, R., and Frotscher, M. (1992). Reduction of posttraumatic transneuronal “early gene” activation and dendritic atrophy by the N-methyl-D-aspartate receptor antagonist MK-801. *Proc. Natl. Acad. Sci. USA* **89**, 5197–5200.
- O'Connor, L.T., Lauterborn, J.C., Smith, M.A., and Gall, C.M. (1995). Expression of agrin mRNA is altered following seizures in adult rat brain. *Mol. Brain Res.* **33**, 277–287.
- O'Connor, L.T., Lauterborn, J.C., Gall, C.M., and Smith, M.A. (1994). Localization and alternative splicing of agrin mRNA in adult rat brain: Transcripts encoding isoforms that aggregate acetylcholine receptors are not restricted to cholinergic regions. *J. Neurosci.* **14**, 1141–1152.
- Phillips, L.L., Lyeth, B.G., Hamm, R.J., and Povlishock, J.T. (1994). Combined fluid percussion brain injury and entorhinal cortical lesion: A model for assessing the interaction between neuroexcitation and deafferentation. *J. Neurotrauma* **11**, 641–656.
- Phillips, L.L., Lyeth, B.G., Hamm, R.J., Reeves, T.M., and Povlishock, J.T. (1998). Glutamate antagonism during secondary deafferentation enhances cognition and axo-dendritic integrity after traumatic brain injury. *Hippocampus* **8**, 390–401.
- Phillips, L.L., and Reeves, T.M. (2001). Interactive pathology following traumatic brain injury modifies hippocampal plasticity. *Restor. Neurol. Neurosci.* **19**, 213–235.
- Povlishock, J.T., and Christman, C.W. (1995). Diffuse axonal injury, in: Waxman, S.G., Kocsis, J.D., Stys, P.K. (eds). *The Axon*. Oxford University Press: New York, pps. 504–529.
- Reif, R., Sales, S., Hettwer, S., Dreier, B., Gisler, C., Wolfel, J., Luscher, D., Zurlinden, A., Stephan, A., Ahmed, S., Baici, A., Ledermann, B., Kunz, B., and Sonderegger, P. (2007). Specific cleavage of agrin by neurotrypsin, a synaptic protease linked to mental retardation. *FASEB J.* **21**, 3468–3478.
- Rupp, F., Payan, D.G., Magill-Solc, C., Cowan, D.M., and Scheller, R.H. (1991). Structure and expression of rat agrin. *Neuron* **6**, 811–823.
- Scheff, S.W., Price, D.A., Hicks, R.R., Baldwin, S.A., Robinson, S., and Brackney, C. (2005). Synaptogenesis in the hippocampal CA1 field following traumatic brain injury. *J. Neurotrauma* **22**, 719–732.

AGRIN EXPRESSION DURING SYNAPTOGENESIS INDUCED BY TBI

- Serpinskaya, A.S., Feng, G., Sanes, J.R., and Craig, A.M. (1999). Synapse formation by hippocampal neurons from agrin-deficient mice. *Dev. Biol.* **205**, 65–78.
- Smith, M.A., and Hilgenberg, L.G.W. (2002). Agrin in the CNS: a protein in search of a function? *Neuroreport* **13**, 1485–1495.
- Sole, S., Petegnief, V., Gorina, R., Chamorro, A., and Planas, A.M. (2004). Activation of matrix metalloproteinase-3 and agrin cleavage in cerebral ischemia/reperfusion. *J. Neuropathol. Exp. Neurol.* **63**, 338–349.
- Steward, O. (1989). Reorganization of neuronal connections following CNS trauma: principles and experimental paradigms. *J. Neurotrauma* **6**, 99–152.
- Steward, O., Vinsant, S.L., and Davis, L. (1988). The process of reinnervation in the dentate gyrus of adult rats: an ultrastructural study of changes in presynaptic terminals as a result of sprouting. *J. Comp. Neurol.* **267**, 203–210.
- Szklarczyk, A., Lapinska, J., Rylski, M., McKay, R.D., and Kaczmarek, L. (2002). Matrix metalloproteinase-9 undergoes expression and activation during dendritic remodeling in adult hippocampus. *J. Neurosci.* **267**, 203–210.
- Thomas, W.S., O'Dowd, D.K., and Smith, M.A. (1993). Developmental expression and alternative splicing of chick agrin RNA. *Dev. Biol.* **158**, 523–535.
- Thompson, S.N., Gibson, T.R., Thompson, B.M., Deng, Y., and Hall, E.D. (2006). Relationship of calpain-mediated proteolysis to the expression of axonal and synaptic plasticity markers following traumatic brain injury in mice. *Exp. Neurol.* **201**, 253–265.
- Tournell, C.E., Bergstrom, R.A., and Ferreira, A. (2006). Progesterone-induced agrin expression in astrocytes modulates glia-neuron interactions leading to synapse formation. *Neuroscience* **141**, 1327–1338.
- Tsen, G., Halfter, W., Kroger, S., and Cole, G.J. (1995). Agrin is a heparan sulfate proteoglycan. *J. Biol. Chem.* **270**, 3392–3399.
- Yang, J-F., Cao, G., Koirala, S., Reddy, L.V., and Ko, C-P. (2001). Schwann cells express active agrin and enhance aggregation of acetylcholine receptors on muscle fibers. *J. Neurosci.* **21**, 9572–9584.
- Yong, V.W., Power, C., Forsyth, P., and Edwards, D.R. (2001). Metalloproteinases in biology and pathology of the nervous system. *Nat. Rev. Neurosci.* **2**, 502–511.
- Yoshimura, S., Teramoto, T., Whalen, M.J., Irizarry, M.C., Takagi, Y., Qui, J., Harada, J., Waeber, C., Breakfield, X.O., and Moskowitz, M.A. (2003). FGF-2 regulates neurogenesis and degeneration in the dentate gyrus after traumatic brain injury in mice. *J. Clin. Invest.* **112**, 1202–1210.

Address reprint requests to:

Linda L. Phillips, Ph.D.

Department of Anatomy and Neurobiology

P.O. Box 980709

School of Medicine

Virginia Commonwealth University Medical Center

Richmond, VA 23298

E-mail: llphilli@vcu.edu